

Reflectionless and Equiscattering Quantum Graphs and Their Applications

Taksu Cheon

Laboratory of Physics

Kochi University of Technology

Tosa Yamada, Kochi 782-8502, Japan

Email: taksu.cheon@kochi-tech.ac.jp

Abstract—The inverse scattering problem of a quantum star graph is shown to be solvable as a diagonalization problem of Hermitian unitary matrix when the connection condition is given by scale invariant Fulop-Tsutsui form. This enables the construction of quantum graphs with desired properties. The quantum vertices with uniform and reflectionless scatterings are examined, and their finite graph approximations are constructed. It is shown that a controllable spectral filter can be constructed from a certain reflectionless graph with the application of external potential on a line.

Keywords—quantum graph; singular vertex; quantum wire; inverse scattering; quantum filter

I. INTRODUCTION

The inverse scattering is one of the most intriguing problems in quantum mechanics. The inverse scattering problem of quantum graph [1], [2], [3], [4], in particular, has two aspects. Because the quantum graph is a nontrivial solvable system [5], it presents a challenge for extending the range of solvable inverse scattering problems. It is also increasingly becoming important as the design principle of single electron devices based on nanoscale quantum wires.

In this article, we consider the inverse scattering problem on a star graph with Fulop-Tsutsui vertices [6], the scale invariant subset of most general vertex couplings [7]. A star graph is the elementary building block of generic graph having many half-lines connected together at a single point, the singular vertex. The scattering matrix of star graph with Fulop-Tsutsui condition is energy independent. We exploit this simplicity to give the full answer to its inverse scattering problem in the form of *diagonalization problem of Hermitian unitary matrix*. Two special examples of inverse scattering problems, that of reflectionless transmission, and of equal-scattering including the reflection, are examined in detail. Very interesting designs involving Diophantine numbers emerge for the realization of quantum device with such properties. Since any singular vertex is effectively reduced to Fulop-Tsutsui vertex in both high and low energy limits [8], our study hopefully opens up a door for the full study of inverse scattering problems for general singular vertex.

The quantum graph has to be controllable by external field of macroscopic scale, if it is to be useful as a quantum device. We formulate scattering problems on a quantum graph with constant potentials with differing strengths applied to graph

lines. The formalism is applied to analyze several models of quantum graphs with external potential on a line. The existence of threshold resonance phenomenon is pointed out, and it is shown to be useful in designing controllable spectral filtering devices. Specifically, a controllable band filter with flat spectral response is constructed from a $n = 4$ reflectionless quantum graph.

This article is organized as follows: In the second section, we formulate the inverse scattering problem of scale invariant graph vertices in terms of matrix diagonalization. In the third section, a scheme to approximate the vertex with small structures made up of δ -vertices is developed. In the fourth section, the scheme is applied to obtain reflectionless and equitransmitting quantum graphs. The accuracy of the approximating procedure is also examined in the same section. In the fifth section, with the application of the quantum graphs as controllable quantum devices in mind, the scattering formalism is extended to handle the added external potentials on the lines. In the sixth section, we take a look at the threshold resonance phenomenon which is found in the quantum graph with a line subjected to the added potential. In the seventh section, we examine a $n = 4$ reflectionless graph with a positive external potential on a line, and point out its utility as band spectral filter. The paper ends with the concluding eighth section.

II. INVERSE SCATTERING AS DIAGONALIZATION

The quantum graph is a system made up of interconnected one-dimensional lines on which a quantum particle moves around. The simplest nontrivial quantum graph is a star-shaped graph with a single node. This “elementary particle of quantum graph” is also referred to as singular quantum vertex. We start by considering a singular quantum vertex of degree n , having n half-lines coming out of a point-like node (Fig. 1). The quantum particle moving on i -th line is described by the wave function $\psi_i(x_i)$ which satisfies the Schrödinger equation, which, after proper rescaling of the units, read

$$-\frac{d^2}{dx_i^2}\psi_i(x_i) = k^2\psi_i(x_i) \quad (i = 1, \dots, n). \quad (1)$$

The coordinates x_i on the i -th line are labeled outwardly from the singular vertex, which is assigned the value $x_i = 0$ for all i . The specification of the connection condition at the node

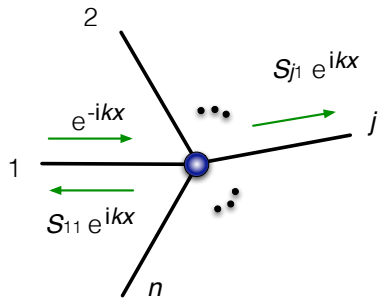


Fig. 1. Schematic representation of scattering of a quantum particle on a star graph of degree n .

$x_i = 0$ characterizes the system. Let us define the boundary vectors Ψ and Ψ' by

$$\Psi = \begin{pmatrix} \psi_1(0) \\ \vdots \\ \psi_n(0) \end{pmatrix}, \quad \Psi' = \begin{pmatrix} \psi'_1(0) \\ \vdots \\ \psi'_n(0) \end{pmatrix}, \quad (2)$$

in which $\psi'_i(x_i)$ is the spatial derivative of the wave function on i -th line. The current conservation at the node can be expressed as

$$\Psi^\dagger \Psi' - \Psi'^\dagger \Psi = 0. \quad (3)$$

It is shown in [7] that this condition can be rephrased as

$$A\Psi + B\Psi' = 0. \quad (4)$$

with two $n \times n$ matrices A and B , which satisfy

$$A^\dagger B = B^\dagger A, \quad \text{rank}(A, B) = n. \quad (5)$$

It is shown in [9] that this most general connection condition is characterized by a complex matrix T of size $(n-m) \times m$ where m can take the integer value $m = 1, 2, \dots, n-1$, and is given by

$$\begin{pmatrix} I^{(m)} & T \\ 0 & 0 \end{pmatrix} \Psi' = \begin{pmatrix} S & 0 \\ -T^\dagger & I^{(n-m)} \end{pmatrix} \Psi, \quad (6)$$

where S is a Hermitian matrix of size $m \times m$. The scale invariant subfamily of most general connection condition is characterized by a complex matrix T of size $(n-m) \times m$ where m can take the integer value $m = 1, 2, \dots, n-1$, and is given by

$$\begin{pmatrix} I^{(m)} & T \\ 0 & 0 \end{pmatrix} \Psi' = \begin{pmatrix} 0 & 0 \\ -T^\dagger & I^{(n-m)} \end{pmatrix} \Psi, \quad (7)$$

where $I^{(l)}$ signifies the identity matrix of size $l \times l$. To achieve the form (7), we may have to suitably renumber lines, in general.

The particle coming in from the j -th line and scattered off the singular vertex is described by the scattering wave function on the i -th line, $\psi_i^{(j)}(x)$ which is given in the form

$$\begin{aligned} \psi_i^{(j)}(x) &= e^{-ikx} + S_{jj} e^{ikx} & (i = j) \\ &= S_{ij} e^{ikx} & (i \neq j). \end{aligned} \quad (8)$$

Consider matrices $M = \{\psi_{ij}(0)\}$ and $M' = \{\psi'_{ij}(0)\}$. They are given, in terms of \mathcal{S} by

$$M = I^{(n)} + \mathcal{S}, \quad M' = ik(-I^{(n)} + \mathcal{S}), \quad (9)$$

Since each column of M and M' satisfies the equation (7), we have

$$\begin{pmatrix} I^{(m)} & T \\ 0 & 0 \end{pmatrix} M' = \begin{pmatrix} 0 & 0 \\ -T^\dagger & I^{(n-m)} \end{pmatrix} M. \quad (10)$$

From (9) and (10), we easily obtain the explicit solution of the scattering matrix $\mathcal{S} = \{S_{i,j}\}$ in the form

$$\mathcal{S} = -I^{(n)} + 2 \begin{pmatrix} I^{(m)} \\ T^\dagger \end{pmatrix} \left(I^{(m)} + TT^\dagger \right)^{-1} \begin{pmatrix} I^{(m)} & T \end{pmatrix}. \quad (11)$$

Squared moduli of the elements of \mathcal{S} have the following interpretation: $|S_{ij}|^2$ for $j \neq i$ represents the probability of transmission from the i -th to the j -th line, $|S_{jj}|^2$ is the probability of reflection on the j -th line. A notable feature of this \mathcal{S} obtained from Fulop-Tsutsui vertex its Hermiticity;

$$\mathcal{S}^\dagger = \mathcal{S}. \quad (12)$$

Since the scattering matrix is unitary for any system, in general, *i. e.*

$$\mathcal{S}^\dagger \mathcal{S} = I^{(n)}, \quad (13)$$

\mathcal{S} belongs to a special class of square matrix that is at the same time *Hermitian and unitary* [10].

A natural question to be asked is what subset of Hermitian and unitary matrix, the scattering matrix of entire Fulop-Tsutsui vertex forms. To answer this question, we look for an alternative expression of (11). By multiplying $\begin{pmatrix} I^{(m)} & T \end{pmatrix}$ from the left, we obtain

$$\begin{pmatrix} I^{(m)} & T \end{pmatrix} \mathcal{S} = \begin{pmatrix} I^{(m)} & T \end{pmatrix} \quad (14)$$

Similarly, by multiplying $\begin{pmatrix} T^\dagger & I^{(n-m)} \end{pmatrix}$ from the left, we obtain

$$\begin{pmatrix} T^\dagger & I^{(n-m)} \end{pmatrix} \mathcal{S} = -\begin{pmatrix} T^\dagger & I^{(n-m)} \end{pmatrix}. \quad (15)$$

Combining these two expressions, we have $X_m \mathcal{S} = Z_m X_m$ with the definitions

$$\begin{aligned} X_m &= \begin{pmatrix} I^{(m)} & T \\ T^\dagger & -I^{(n-m)} \end{pmatrix}, \\ Z_m &= \begin{pmatrix} I^{(m)} & 0 \\ 0 & -I^{(n-m)} \end{pmatrix}. \end{aligned} \quad (16)$$

Thus we can express \mathcal{S} in the form of a product of three Hermitian matrices as [10]

$$\mathcal{S} = X_m^{-1} Z_m X_m. \quad (17)$$

Interestingly, (17) can also be viewed as the diagonalization of Hermitian unitary matrix \mathcal{S} by a non-unitary Hermitian matrix X_m . We can show, in fact, that this form leads to the path to the inverse scattering problem for quantum graph vertex of Fulop-Tsutsui type: Let us suppose that the full set of scattering data is given in terms of an arbitrary Hermitian

unitary matrix \mathcal{S} . Let us signify the rank of the matrix $\mathcal{S} + I^{(n)}$ by m . After proper renumbering of lines, we can write this matrix in the form

$$\mathcal{S} + I^{(n)} = \begin{pmatrix} I^{(m)} \\ T^\dagger \end{pmatrix} M \begin{pmatrix} I^{(m)} & T \end{pmatrix}, \quad (18)$$

where M is a Hermitian $m \times m$ matrix, and T , a complex $(n - m) \times m$ matrix. From the unitarity of \mathcal{S} , we find the relation $(\mathcal{S} + I^{(n)})^2 = 2(\mathcal{S} + I^{(n)})$, from which we obtain

$$M = 2(I^{(m)} + TT^\dagger)^{-1}, \quad (19)$$

and we therefore arrive at (11). We conclude, therefore, that *any Hermitian unitary matrix can be viewed as a scattering matrix \mathcal{S} of a Fulop-Tsutsui vertex.*

In order for a quantum star graph to break scale invariance and obtain k -dependence, its scattering matrix needs to become non-Hermite. The existence and the uniqueness of the inverse scattering solution of quantum star graph extend to this more general non-Hermite case also. These observations can be reached easily and directly from the original ‘‘U-form’’ of connection condition using a unitary matrix [2], [7], but our procedure holds definite advantage of giving us T directly, which is known [9] to allow us the physical construction of a finite quantum graph whose small size limit reproduces the prescribed \mathcal{S} .

The procedure of diagonalization, in practice, is quite cumbersome for large n . A simpler alternative to obtain T from \mathcal{S} is the following: Let us divide \mathcal{S} into four submatrices \mathcal{S}_{11} , \mathcal{S}_{12} , \mathcal{S}_{21} and \mathcal{S}_{22} of size $m \times m$, $m \times (n - m)$, $(n - m) \times m$ and $(n - m) \times (n - m)$, respectively as

$$\mathcal{S} = \begin{pmatrix} \mathcal{S}_{11} & \mathcal{S}_{12} \\ \mathcal{S}_{21} & \mathcal{S}_{22} \end{pmatrix}. \quad (20)$$

These submatrices have the properties

$$\mathcal{S}_{11}^\dagger = \mathcal{S}_{11}, \quad \mathcal{S}_{22}^\dagger = \mathcal{S}_{22}, \quad \mathcal{S}_{21}^\dagger = \mathcal{S}_{12}, \quad (21)$$

and also

$$\begin{aligned} \mathcal{S}_{11}^2 + \mathcal{S}_{12}^2 &= I^{(m)}, \\ \mathcal{S}_{22}^2 + \mathcal{S}_{21}^2 &= I^{(n-m)}, \\ \mathcal{S}_{11}\mathcal{S}_{12} + \mathcal{S}_{12}\mathcal{S}_{22} &= 0. \end{aligned} \quad (22)$$

From these equations, we have the explicit expressions of T in terms of \mathcal{S}_{ij} ;

$$\begin{aligned} T &= \left(I^{(m)} + \mathcal{S}_{11} \right)^{-1} \mathcal{S}_{12} \\ &= \mathcal{S}_{21}^\dagger \left(I^{(n-m)} - \mathcal{S}_{22} \right)^{-1}. \end{aligned} \quad (23)$$

It is easy to check that the forms (11) and (17) can be kept under the index renumbering $\alpha \leftrightarrow \beta$ both for $\alpha, \beta \leq m$ and for $\alpha, \beta > m$ with the proper transformation for the elements of T ; It is given by $t_{\alpha j} \leftrightarrow t_{\beta j}$ for the former and $t_{i\alpha} \leftrightarrow t_{i\beta}$

for the latter. For the case of $\alpha \leq m$ and $\beta > m$, it is given by $t_{ij} \rightarrow t'_{ij}$ with

$$t'_{ij} = \frac{t_{ij}t_{\alpha\beta} - t_{\alpha j}t_{i\beta} \bar{\delta}_{i\alpha} \bar{\delta}_{j\beta}}{t_{\alpha\beta} - \frac{t_{\alpha j} \delta_{i\alpha} - \delta_{\alpha j} t_{i\alpha} + \delta_{i\alpha} \delta_{j\beta}}{t_{\alpha\beta}}}, \quad (24)$$

where we define $\bar{\delta}_{ij} = 1 - \delta_{ij}$. This implies that it is not possible to exchange the indices α and β whose $t_{\alpha\beta}$ is zero. This corresponds to the index ordering for which both $(I^{(m)} + \mathcal{S}_{11})$ and $(I^{(n-m)} - \mathcal{S}_{22})$ are singular and the T is undefined, thus the boundary condition at the singular vertex does not take the form (7).

III. FINITE APPROXIMATION

Finite tubes connected at a node generically tend, in their small diameter limit, to a vertex with delta-like connections, given by $m = 1$, and $T = \begin{pmatrix} 1 & \cdots & 1 \end{pmatrix}$, namely

$$\begin{pmatrix} 1 & 1 & \cdots & 1 \\ 0 & 0 & \cdots & 0 \\ \vdots & & \ddots & \\ 0 & 0 & \cdots & 0 \end{pmatrix} \Psi' = \begin{pmatrix} v & 0 & \cdots & 0 \\ 0 & 1 & & 0 \\ \vdots & & \ddots & \vdots \\ 0 & 0 & \cdots & 1 \end{pmatrix} \Psi, \quad (25)$$

and very often to its strength zero limit, $v = 0$, a free vertex [11]. We might also consider applying localized magnetic field to achieve phase change. It is natural, therefore, to devise a design principle to construct arbitrary connection condition out of this elementary vertex. Once all elements of $T = \{t_{ij}\}$, $i = 1, \dots, m$ and $j = m + 1, \dots, n$, are obtained, a finite graph with internal lines and the δ -coupling vertices can be constructed systematically, whose small-size limit reproduces the boundary condition of Fulop-Tsutsui vertex, (7). The scheme developed in [12] works as follows.

(i) Assemble the edges of n half lines which we assign the numbers $j = 1, 2, \dots, n$, and connect them in pairs (i, j) by internal lines of length d/r_{ij} except when $r_{ij} = 0$, for which case, the pairs are left unconnected. Apply vector potential A_{ij} on the line (i, j) to produce extra phase shift χ_{ij} between the edges when its value is nonzero. Place δ potential of strength v_i at each edge i .

(ii) The length ratio r_{ij} and the phase shift χ_{ij} are determined from the non-diagonal elements of the matrix Q defined by

$$Q = \begin{pmatrix} T \\ I^{(n-m)} \end{pmatrix} \begin{pmatrix} -T^\dagger & I^{(m)} \end{pmatrix} = \begin{pmatrix} -TT^\dagger & T \\ -T^\dagger & I^{(m)} \end{pmatrix}, \quad (26)$$

by the relation $r_{ij}e^{i\chi_{ij}} = Q_{ij}$ ($i \neq j$). This means that we have

$$\begin{aligned} r_{ij}e^{i\chi_{ij}} &= - \sum_{l>m} t_{il}t_{jl}^* & (i, j \leq m), \\ &= t_{ij} & (i \leq m, j > m), \\ &= 0 & (i, j > m). \end{aligned} \quad (27)$$

(iii) The strength v_i is given by the diagonal elements of the matrix V defined by

$$V = \frac{1}{d}(2I^{(n)} - J^{(n)})R, \quad (28)$$

where R is the matrix whose elements are made from absolute values of matrix elements of Q , i.e.

$$R = \{r_{ij}\} = \{|Q_{ij}|\}. \quad (29)$$

The matrix $J^{(n)}$ is of size $n \times n$ with all elements given by 1. This means that we have

$$\begin{aligned} v_i &= \frac{1}{d}\left(1 - \sum_{l \leq m} r_{li}\right) & (i > m), \\ &= \frac{1}{d}\left(\sum_{l > m} [r_{il}^2 - r_{il}] - \sum_{l \neq i, l \leq m} r_{il}\right) & (i \leq m). \end{aligned} \quad (30)$$

These fine tunings of length and strength are necessary to counter the generic opaqueness brought in with every addition of vertices and lines into a graph.

The wave function $\phi(x) = \phi_{i,j}(x)$ on any internal line (i, j) , we have the relation

$$\begin{pmatrix} \phi'(0) \\ e^{ix}\phi(\frac{d}{r}) \end{pmatrix} = -\frac{r}{d} \begin{pmatrix} F(\frac{d}{r}) & -G(\frac{d}{r}) \\ G(\frac{d}{r}) & -F(\frac{d}{r}) \end{pmatrix} \begin{pmatrix} \phi(0) \\ e^{ix}\phi(\frac{d}{r}) \end{pmatrix}, \quad (31)$$

with $F(x) = x \cot x$ and $G(x) = x \operatorname{cosec} x$. Combining (31) with the condition at the i -th endpoint,

$$\psi'_i(0) + \sum_{j \neq i} \phi'_{ij}(0) = v_i \psi_i(0) \quad (32)$$

where we have the δ -potential of strength v_i , we obtain the relations between the boundary values $\psi_i = \psi_i(0)$ and $\psi'_i = \psi'_i(0)$ in the form

$$d\psi'_i = \left(v_i d + \sum_{l \neq i} r_{il} F_{il} \right) \psi_i - \sum_{l \neq i} e^{ix_{ij}} r_{il} G_{il} \psi_l, \quad (33)$$

where the obvious notations $F_{ij} = \frac{d}{r_{il}} \cot \frac{d}{r_{il}}$ and $G_{ij} = \frac{d}{r_{il}} \operatorname{cosec} \frac{d}{r_{il}}$ are adopted. Note that the equation (33) is exact and does not involve any approximation. In the short range limit $d \rightarrow 0$, we have $F_{ij} = 1 + O(d^2)$ and $G_{ij} = 1 + O(d^2)$. We can then show, with a straightforward calculation in the manner of [9], that the limit $d \rightarrow 0$ gives the desired connection condition for Fulop-Tsutsui vertex (7).

IV. REFLECTIONLESS AND EQUISCATTERING GRAPHS

With the solution of the inverse scattering fully formulated, it is now possible to find a Fulop-Tsutsui vertex from a given scattering matrix with specific requirement. Our previous results detailed in [12] showing the reconstruction of ‘‘Free-like’’ scattering is one such example, and could have been achieved easier with current method. We now ask whether there is fully reflectionless graph whose scattering matrix has only zeros for its diagonal elements, $\mathcal{S}_{ii} = 0$. Vertices yielding such scattering matrix is known to be useful in developing semiclassical theory of quantum spectra [13]. If we

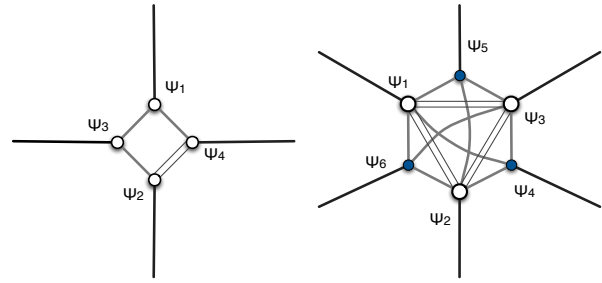


Fig. 2. Finite approximation to the reflectionless Fulop-Tsutsui vertices corresponding to (35) (left) and (41) (right) constructed according to (26)-(28). The relative length of internal lines r_{ij} and strength of the δ -potentials v_j for former are given by (40), while those for the latter are given by (43). Double lines indicate the existence of non-zero phase shift χ_{ij} .

limit ourselves to real \mathcal{S} , it becomes symmetric matrix with $\mathcal{S}_{ij} = \mathcal{S}_{ji}$.

We note a useful relation concerning the trace of the scattering matrix. Taking the trace of (17) and utilizing $\operatorname{tr}(AB) = \operatorname{tr}(BA)$, we have

$$\operatorname{tr} \mathcal{S} = \operatorname{tr} Z_m = 2m - n. \quad (34)$$

Since \mathcal{S} for reflectionless scattering is traceless, we can have such scattering only for $n = 2m$.

Our first example is with $n = 4$ whose \mathcal{S} is given by

$$\mathcal{S} = \begin{pmatrix} 0 & 0 & a & \sqrt{1-a^2} \\ 0 & 0 & \sqrt{1-a^2} & -a \\ a & \sqrt{1-a^2} & 0 & 0 \\ \sqrt{1-a^2} & -a & 0 & 0 \end{pmatrix}, \quad (35)$$

and the corresponding T , by

$$T = \begin{pmatrix} a & \sqrt{1-a^2} \\ \sqrt{1-a^2} & -a \end{pmatrix}. \quad (36)$$

The finite approximation is characterized by

$$r_{12} = r_{34} = 0, \quad r_{13} = r_{24} = a, \quad r_{23} = r_{14} = \sqrt{1-a^2},$$

$$e^{ix_{24}} = -1, \quad e^{ix_{ij}} = 1 \text{ all others,}$$

$$v_1 = v_2 = v_3 = v_4 = \frac{1-a-\sqrt{1-a^2}}{d}, \quad (37)$$

The finite graph approximation is schematically illustrated in the left side of Figure 1.

We next turn to reflectionless scattering with uniform transmission to all other lines. The smallest non-trivial example of such matrix exists for $n = 4$, and given by

$$\mathcal{S} = \frac{1}{\sqrt{5}} \begin{pmatrix} 0 & 1 & 1 & 1 \\ 1 & 0 & -i & i \\ 1 & i & 0 & -i \\ 1 & -i & i & 0 \end{pmatrix}. \quad (38)$$

The corresponding T is given by

$$T = \begin{pmatrix} \omega & \omega^{-1} \\ \omega^{-4} & \omega^4 \end{pmatrix}. \quad (39)$$

with $\omega = e^{i\frac{\pi}{6}}$. Our finite approximation is specified by following numbers.

$$\begin{aligned} r_{13} = r_{14} = r_{23} = r_{24} = 1, \quad r_{12} = r_{34} = 0, \\ e^{i\chi_{13}} = e^{i\frac{\pi}{6}}, e^{i\chi_{14}} = e^{-i\frac{\pi}{6}}, e^{i\chi_{23}} = e^{-4i\frac{\pi}{6}}, e^{i\chi_{24}} = e^{4i\frac{\pi}{6}}, \\ v_1 = v_2 = v_3 = v_4 = -\frac{1}{d}, \end{aligned} \quad (40)$$

The finite graph approximation is schematically illustrated in the right side of Figure 1.

If we limit ourselves to real scattering matrix, such matrix, called *symmetric conference matrix*, is known to exist for $n = 6, 10, 14, 18, 26, 30, 38, \dots$. We look at the example of $n = 6$ whose \mathcal{S} is given by

$$\mathcal{S} = \frac{1}{\sqrt{5}} \begin{pmatrix} 0 & -1 & -1 & -1 & 1 & 1 \\ -1 & 0 & -1 & 1 & -1 & 1 \\ -1 & -1 & 0 & 1 & 1 & -1 \\ -1 & 1 & 1 & 0 & 1 & 1 \\ 1 & -1 & 1 & 1 & 0 & 1 \\ 1 & 1 & -1 & 1 & 1 & 0 \end{pmatrix}. \quad (41)$$

The corresponding T is given by

$$T = \begin{pmatrix} 1 & 1 + \gamma & 1 + \gamma \\ 1 + \gamma & 1 & 1 + \gamma \\ 1 + \gamma & 1 + \gamma & 1 \end{pmatrix}. \quad (42)$$

where $\gamma = (\sqrt{5} - 1)/2$ is the golden mean. Our finite approximation is specified by following numbers.

$$\begin{aligned} r_{12} = r_{23} = r_{13} = 4 + 3\gamma, \quad r_{14} = r_{25} = r_{36} = 1, \\ r_{15} = r_{16} = r_{26} = r_{24} = r_{31} = r_{32} = 1 + \gamma, \\ r_{45} = r_{46} = r_{56} = 0, \\ e^{i\chi_{12}} = e^{i\chi_{23}} = e^{i\chi_{13}} = -1, \quad e^{i\chi_{ij}} = 1 \text{ all others}, \\ v_1 = v_2 = v_3 = -6\frac{\gamma + 1}{d}, \quad v_4 = v_5 = v_6 = -2\frac{\gamma + 1}{d}. \end{aligned} \quad (43)$$

The finite graph approximation is schematically illustrated in the right side of Figure 1.

Our next example is the reflectionless equitransmitting graph with $n = 10$, that corresponds to the \mathcal{S} matrix given by $n = 10$ conference matrix

$$\mathcal{S} = \frac{1}{3} \begin{pmatrix} 0 & -1 & 1 & 1 & -1 & -1 & 1 & 1 & 1 & 1 \\ -1 & 0 & -1 & 1 & 1 & 1 & -1 & 1 & 1 & 1 \\ 1 & -1 & 0 & -1 & 1 & 1 & 1 & -1 & 1 & 1 \\ 1 & 1 & -1 & 0 & -1 & 1 & 1 & 1 & -1 & 1 \\ -1 & 1 & 1 & -1 & 0 & 1 & 1 & 1 & 1 & -1 \\ -1 & 1 & 1 & 1 & 1 & 0 & 1 & -1 & -1 & 1 \\ 1 & -1 & 1 & 1 & 1 & 1 & 0 & 1 & -1 & -1 \\ 1 & 1 & -1 & 1 & 1 & -1 & 1 & 0 & 1 & -1 \\ 1 & 1 & 1 & -1 & 1 & -1 & -1 & 1 & 0 & 1 \\ 1 & 1 & 1 & 1 & -1 & 1 & -1 & -1 & 1 & 0 \end{pmatrix} \quad (44)$$

The trace of \mathcal{S} is zero again, and we have $m = \frac{n}{2} = 5$. The matrix T specifying the vertex is given by

$$T = \begin{pmatrix} -1 & 0 & 1 & 1 & 0 \\ 0 & -1 & 0 & 1 & 1 \\ 1 & 0 & -1 & 0 & 1 \\ 1 & 1 & 0 & -1 & 0 \\ 0 & 1 & 1 & 0 & -1 \end{pmatrix}, \quad (45)$$

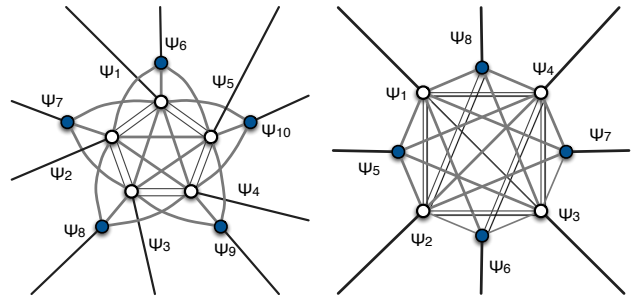


Fig. 3. Finite approximation to the equal-scattering Fulop-Tsutsui vertex corresponding to $n = 10$ conference matrix, (44) (left) and $n = 8$ Hadamard matrix, (47) (right) constructed according to (26)-(28). The relative length of internal lines r_{ij} and strength of the δ -potentials v_j for former are given by (46), while those for the latter are given by (49). Double lines indicate the existence of non-zero phase shift χ_{ij} .

where $\sigma = \sqrt{2} - 1$ is the silver mean. Our finite approximation is specified by following numbers for vertices;

$$\begin{aligned} r_{12} = r_{23} = r_{34} = r_{45} = r_{15} = 1, \\ r_{16} = r_{27} = r_{38} = r_{49} = r_{5a} = 1, \\ r_{18} = r_{29} = r_{3a} = r_{46} = r_{57} = 1, \\ r_{19} = r_{2a} = r_{36} = r_{47} = r_{58} = 1, \\ r_{13} = r_{14} = r_{24} = r_{25} = r_{35} = 2, \\ r_{17} = r_{28} = r_{39} = r_{4a} = r_{56} = 0, \\ r_{1a} = r_{26} = r_{37} = r_{48} = r_{59} = 0, \\ r_{67} = r_{78} = r_{89} = r_{9a} = r_{6a} = 0, \\ r_{68} = r_{79} = r_{8a} = r_{69} = r_{7a} = 0, \\ e^{i\chi_{12}} = e^{i\chi_{23}} = e^{i\chi_{34}} = e^{i\chi_{45}} = e^{i\chi_{15}} = -1 \\ e^{i\chi_{16}} = e^{i\chi_{27}} = e^{i\chi_{38}} = e^{i\chi_{49}} = e^{i\chi_{5a}} = -1 \\ e^{i\chi_{ij}} = 1 \text{ all others}, \\ v_1 = v_2 = v_3 = v_4 = v_5 = -\frac{6}{d}, \\ v_6 = v_7 = v_8 = v_9 = v_a = -\frac{2}{d}. \end{aligned} \quad (46)$$

Here, a in subscript stands for the index for 10th edge. The finite graph approximation for this case is schematically illustrated in the left side of Figure 2.

The last example is the equal-scattering graph, in which in the scattering is uniform in all lines including the line of incoming particle. Such matrix, called *symmetric Hadamard matrix*, is known to exist for $n = 2^k, k = 0, 1, \dots$. An example of such \mathcal{S} for $n = 8$ is given by

$$\mathcal{S} = \frac{1}{\sqrt{8}} \begin{pmatrix} 1 & -1 & -1 & -1 & -1 & 1 & 1 & 1 \\ -1 & 1 & -1 & -1 & 1 & -1 & 1 & 1 \\ -1 & -1 & 1 & -1 & 1 & 1 & -1 & 1 \\ -1 & -1 & -1 & 1 & 1 & 1 & 1 & -1 \\ 1 & -1 & 1 & 1 & 1 & -1 & 1 & 1 \\ 1 & 1 & -1 & 1 & 1 & 1 & -1 & 1 \\ 1 & 1 & 1 & -1 & 1 & 1 & 1 & -1 \end{pmatrix}. \quad (47)$$

The trace of \mathcal{S} is again zero, and we have $m = \frac{n}{2} = 4$. The

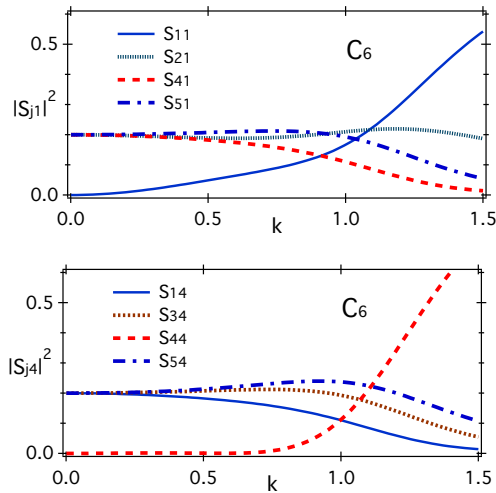


Fig. 4. Scattering probabilities as functions of incoming momentum k (in the unit of $1/d$) of finite quantum graph approximating the equal-transmitting reflectionless vertex with $n = 6$ edges represented in Figure 1, right.

matrix T specifying the Fulop-Tsutsui the vertex is given by

$$T = \frac{1}{\sigma + 1} \begin{pmatrix} \sigma & 1 & 1 & 1 \\ 1 & \sigma & 1 & 1 \\ 1 & 1 & \sigma & 1 \\ 1 & 1 & 1 & \sigma \end{pmatrix}. \quad (48)$$

where $\sigma = \sqrt{2} - 1$ is the silver mean. Our finite approximation is specified by following numbers for verteces;

$$\begin{aligned} r_{12} = r_{13} = r_{14} = r_{23} = r_{24} = r_{34} &= 1 + \sigma, \\ r_{15} = r_{26} = r_{37} = r_{48} &= \frac{\sigma}{1 + \sigma}, \\ r_{16} = r_{17} = r_{18} = r_{27} = r_{28} = r_{38} &= \frac{1}{1 + \sigma}, \\ r_{25} = r_{35} = r_{36} = r_{45} = r_{46} = r_{47} &= \frac{1}{1 + \sigma}, \\ r_{56} = r_{57} = r_{58} = r_{67} = r_{68} = r_{78} &= 0, \\ e^{i\chi_{12}} = e^{i\chi_{13}} = e^{i\chi_{14}} = e^{i\chi_{23}} &= e^{i\phi_{24}} = e^{i\chi_{34}} = -1, \quad e^{i\chi_{ij}} = 1 \text{ all others,} \\ v_1 = v_2 = v_3 = v_4 &= -\frac{5\sigma - 3}{d}, \\ v_5 = v_6 = v_7 = v_8 &= -\frac{\sigma + 1}{d}. \end{aligned} \quad (49)$$

The finite graph approximation is schematically illustrated in the right side of Figure 2.

We now take a look at the convergence of the finite size graph approximation by numerical calculations. In Figure 3, we display the scattering matrix of the finite graph that is constructed to approximate equal-scattering reflectionless matrix, (41). These are calculated directly from (33). The value of the wave length k is in the unit of $1/d$. The convergence can be seen as quite good below $kd \lesssim 0.2$. Numerical analysis of other examples of different graphs give essentially the same conclusion that the construction does represent physical realization of singular Fulop-Tsutsui vertex.

V. SCATTERING MATRIX FOR GRAPH WITH POTENTIALS

We are interested in controlling the scattering properties of a quantum star graph with n lines through the addition of potentials on the lines. Suppose that constant potential U_i is applied to the i -th line. The Schrödinger equation now reads

$$-\frac{d^2}{dx_i^2} \psi_i(x_i) = (k^2 - U_i) \psi_i(x_i) \quad (i = 1, \dots, n). \quad (50)$$

Suppose a quantum particle with mechanical energy E comes in the vertex from the j -th line, and scattered into all the lines through the vertex. The i -th component of the wave function is given by

$$\begin{aligned} \psi_i^{(j)}(x) &= e^{-ik_i x} + \mathcal{S}_{jj} e^{ik_i x} \quad (i = j) \\ &= \sqrt{\frac{k_j}{k_i}} \mathcal{S}_{ij} e^{ik_i x} \quad (i \neq j), \end{aligned} \quad (51)$$

where k_ℓ is the local momentum on the ℓ -th line, defined by

$$k_\ell = \sqrt{E - U_\ell}, \quad (52)$$

where U_ℓ is the potential on the ℓ -th line. The coefficients $\sqrt{k_j/k_i}$ is there to impose proper normalization to guarantee that the flux conservation is given by $\Psi^\dagger \Psi' - \Psi'^\dagger \Psi = 0$ as before. The scattering matrix $\mathcal{S} = \{\mathcal{S}_{ij}\}$ now depends, besides the internal properties of the vertex, on E and U_1, U_2, \dots, U_n .

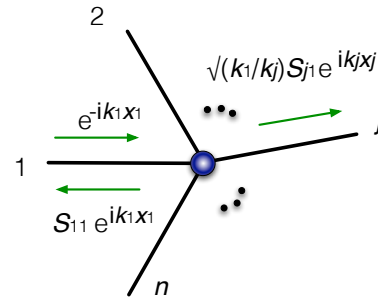


Fig. 5. Schematic representation of scattering of a quantum particle on a star graph of degree n with potentials U_i on the line i .

As before, we define matrices $M = \{\psi_{ij}(0)\}$ and $M' = \{\psi'_{ij}(0)\}$. This time, from (51), we have

$$\begin{aligned} M &= I^{(n)} + K^{-1} S K, \\ M' &= iK^2 (-I^{(n)} + K^{-1} S K), \end{aligned} \quad (53)$$

where the matrix K is defined by its elements

$$K_{ij} = \sqrt{k_i} \delta_{ij}. \quad (54)$$

The boundary condition $AM + BM' = 0$, together with (53) leads to [14]

$$\mathcal{S} = -(AK^{-1} + iBK)^{-1} (AK^{-1} - iBK), \quad (55)$$

which is the desired equation.

VI. THRESHOLD RESONANCE IN STAR GRAPH WITH EXTERNAL POTENTIAL

Let us consider an $n = 3$ star graph with a Fulop-Tsutsui coupling with

$$T = \begin{pmatrix} a & b \end{pmatrix}, \quad (56)$$

which gives the explicit equation for the boundary condition $B\Psi' = -A\Psi$ in the form

$$\begin{pmatrix} 1 & a & b \\ 0 & 0 & 0 \\ 0 & 0 & 0 \end{pmatrix} \Psi' = \begin{pmatrix} 0 & 0 & 0 \\ -a & 1 & 0 \\ -b & 0 & 1 \end{pmatrix} \Psi. \quad (57)$$

The scattering matrix in the absence of potentials $U_i = 0$ is given by

$$S = \frac{1}{1+a^2+b^2} \begin{pmatrix} 1-a^2-b^2 & 2a & 2b \\ 2a & -1+a^2-b^2 & 2ab \\ 2b & 2ab & -1-a^2+b^2 \end{pmatrix}. \quad (58)$$

In order to make the system controllable with external field of macroscopic scale, we add a constant potential to one of the lines [14]. We choose the third line for this purpose, while leaving the other two lines free. The graph is schematically illustrated in Fig. 6. The system is conceived as a model of the quantum device that is controlled through the variation of the potential strength. The roles of individual lines are identified as follows:

- Line 1 is the *input*. Particles of various energies are coming in the vertex along this line.
- Line 2 is the *output*. Particles passed through the vertex are gathered on this line.
- Line 3 is the *controlling line*. We assume that this line is subjected to an adjustable constant external potential U .

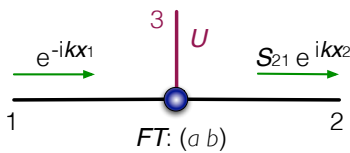


Fig. 6. Schematic depiction of the $n = 3$ star graph with an external potential U on the line 3.

A quantum particle with energy $E = k^2$ coming in the vertex from the input line 1 is scattered at the vertex into all the lines. The scattering amplitudes can be calculated by substituting the matrices A, B from the boundary condition (57) into equation (55), together with the local momenta

$$k_1 = k_2 = k, \quad k_3 = \sqrt{k^2 - U}. \quad (59)$$

For the incoming particles from the line 1, we obtain:

$$S_{21}(k; U) = \frac{2a}{1 + a^2 + b^2 \sqrt{1 - \frac{U}{k^2}}}, \quad (60)$$

$$S_{11}(k; U) = \frac{1 - a^2 - b^2 \sqrt{1 - \frac{U}{k^2}}}{1 + a^2 + b^2 \sqrt{1 - \frac{U}{k^2}}}, \quad (61)$$

$$S_{31}(k; U) = \frac{2b \left(1 - \frac{U}{k^2}\right)^{\frac{1}{4}} \Theta(k - \sqrt{U})}{1 + a^2 + b^2 \sqrt{1 - \frac{U}{k^2}}}. \quad (62)$$

The Heaviside step function $\Theta(k - \sqrt{U})$ in (62) is there to make the expression valid for all energies k^2 , including $k^2 < U$. It represents the absence of the transmission to the line 3 below the threshold momentum

$$k_{\text{th}} = \sqrt{U}. \quad (63)$$

We look at the probability of transmission from the input line 1 into the output line 2, which we denote by $\mathcal{P}(k; U)$, which is given by

$$\mathcal{P}(k; U) = |S_{21}(k; U)|^2. \quad (64)$$

We are interested in its k -dependence, in particular. We have, from (60),

$$\begin{aligned} \mathcal{P}(k; U) &= \frac{4a^2}{\left(1 + a^2 + b^2 \sqrt{1 - \frac{U}{k^2}}\right)^2} \quad (k \geq \sqrt{U}), \\ &= \frac{4a^2}{(1 + a^2)^2 + b^4 \left(\frac{U}{k^2} - 1\right)} \quad (k \leq \sqrt{U}). \end{aligned} \quad (65)$$

We observe that for a given constant potential on the line 3, $\mathcal{P}(k; U)$ as a function of k grows in the interval $(0, \sqrt{U})$, attains its maximum at $k = k_{\text{th}}$, and decreases in the interval (k_{th}, ∞) . In particular, we have

$$\begin{aligned} \mathcal{P}(0; U) &= 0, \\ \mathcal{P}(k_{\text{th}}; U) &= \left(\frac{2a}{1 + a^2}\right)^2, \\ \mathcal{P}(\infty; U) &= \left(\frac{2a}{1 + a^2 + b^2}\right)^2. \end{aligned} \quad (66)$$

If the parameters a, b satisfy

$$b \gg a \geq 1, \quad (67)$$

the function $\mathcal{P}(k; U)$ displays a sharp peak at the threshold momentum k_{th} . Equation (66) implies that the peak attains the highest possible value 1 for $a = 1$. We conclude that, with the choice $b \gg a = 1$, the system has high input to output transmission probability for particles having momenta $k \approx k_{\text{th}}$, and that the transmission is perfect for $k = k_{\text{th}}$, while the transmission probability for other values of k is strongly suppressed. The situation is numerically illustrated in Fig. 7. The quantum graph schematically depicted in Fig. 6 can be therefore used as an adjustable spectral filter, controllable by the potential put on the controlling line 3. We remark that the resonance at the threshold momentum k_{th} is related to the pole of the scattering matrix which is located on the positive real axis at

$$k_{\text{pol}} = \frac{b^2}{\sqrt{b^4 - (1 + a^2)^2}} \sqrt{U} \quad (68)$$

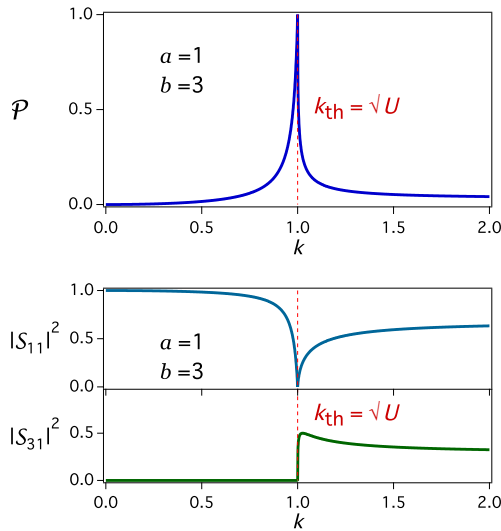


Fig. 7. Scattering characteristics of the graph from Fig. 6 with parameters $a = 1$, $b = 3$. The transmission probability $\mathcal{P}(k; U)$ as a function of k with the value of the potential set to $U = 1$ is plotted in the top figure. The lower figure shows reflection probability $|S_{11}(k; U)|^2$ and the probability of transmission to the controlling line $|S_{31}(k; U)|^2$.

on the unphysical Riemann surface, which is connected to the physical Riemann surface at the cut that runs between $k = \pm k_{th}$.

VII. FLUX CONTROL AND QUANTUM SLUICE-GATE

Let us consider an $n = 4$ star graph, in search of another model of the quantum device, which is schematically illustrated in Fig. 8. The roles of individual lines are identified as follows:

- Line 1 is the *input*. Particles of various energies are coming in the vertex along this line.
- Line 2 is the *output*. Particles passed through the vertex are gathered on this line.
- Line 3 is the *controlling line*. We assume that this line is subjected to an adjustable constant external potential U .
- Line 4 is the *drain*. Our analysis has shown that this seemingly redundant line is needed for the device we wish to construct.

The vertex coupling is again assumed to be of a Fulop-Tsutsui type, specified by the coupling matrix

$$T = \begin{pmatrix} a & a \\ a & -a \end{pmatrix}, \quad (69)$$

which gives the explicit equation for the boundary condition in the form

$$\begin{pmatrix} 1 & 0 & a & a \\ 0 & 1 & a & -a \\ 0 & 0 & 0 & 0 \\ 0 & 0 & 0 & 0 \end{pmatrix} \Psi' = \begin{pmatrix} 0 & 0 & 0 & 0 \\ 0 & 0 & 0 & 0 \\ -a & -a & 1 & 0 \\ -a & a & 0 & 1 \end{pmatrix} \Psi \quad (70)$$

with $a \in \mathbb{R}$. The scattering matrix in the absence of potentials $U = 0$ is given by

$$S = \frac{1}{1+2a^2} \begin{pmatrix} 1-2a^2 & 0 & 2a & 2a \\ 0 & 1-2a^2 & 2a & -2a \\ 2a & 2a & -1+2a^2 & 0 \\ 2a & -2a & 0 & -1+2a^2 \end{pmatrix}. \quad (71)$$

For a particle with energy $E = k^2$ coming in the vertex from

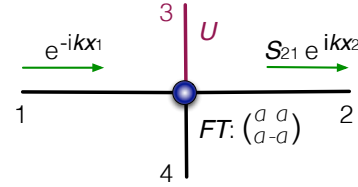


Fig. 8. Schematic depiction of the $n = 4$ star graph with an external potential U on the line No. 3.

the input line 1, we have

$$k_1 = k_2 = k, \quad k_3 = \sqrt{k^2 - U}, \quad k_4 = k. \quad (72)$$

The scattering amplitudes for particles entering from the line 1 can be calculated as

$$S_{21}(k; U) = \frac{2a^2 \left(1 - \sqrt{1 - \frac{U}{k^2}}\right)}{(1+2a^2) \left(1 + 2a^2 \sqrt{1 - \frac{U}{k^2}}\right)}, \quad (73)$$

and

$$S_{11}(k; U) = \frac{1 - 4a^4 \sqrt{1 - \frac{U}{k^2}}}{(1+2a^2) \left(1 + 2a^2 \sqrt{1 - \frac{U}{k^2}}\right)}, \quad (74)$$

$$S_{31}(k; U) = \frac{2a \left(1 - \frac{U}{k^2}\right)^{\frac{1}{4}} \Theta(k - \sqrt{U})}{1 + 2a^2 \sqrt{1 - \frac{U}{k^2}}}, \quad (75)$$

$$S_{41}(k; U) = \frac{2a}{1 + 2a^2}. \quad (76)$$

We again denote the transmission probability from input to output lines by $\mathcal{P}(k; U) = |S_{21}(k; U)|^2$. We obtain, for the transmission below the threshold,

$$\mathcal{P}(k; U) = \frac{4a^4 U / k^2}{(1+2a^2)^2 (1 - 4a^4 + 4a^4 \frac{U}{k^2})} \quad (k \leq \sqrt{U}), \quad (77)$$

and above the threshold,

$$\mathcal{P}(k; U) = \frac{4a^4 \left(1 - \sqrt{1 - \frac{U}{k^2}}\right)^2}{(1+2a^2)^2 \left(1 + 2a^2 \sqrt{1 - \frac{U}{k^2}}\right)^2} \quad (k \geq \sqrt{U}). \quad (78)$$

Hence we have

$$\begin{aligned} \mathcal{P}(0; U) &= \frac{1}{(1+2a^2)^2}, \\ \mathcal{P}(\sqrt{U}; U) &= \frac{4a^4}{(1+2a^2)^2}, \\ \mathcal{P}(\infty; U) &= 0. \end{aligned} \quad (79)$$

When U is fixed, $\mathcal{P}(k; U)$ as a function of k quickly falls off to zero at $k > \sqrt{U}$. A typical behaviour is illustrated in a numerical example in Fig. 9. The peak at the threshold

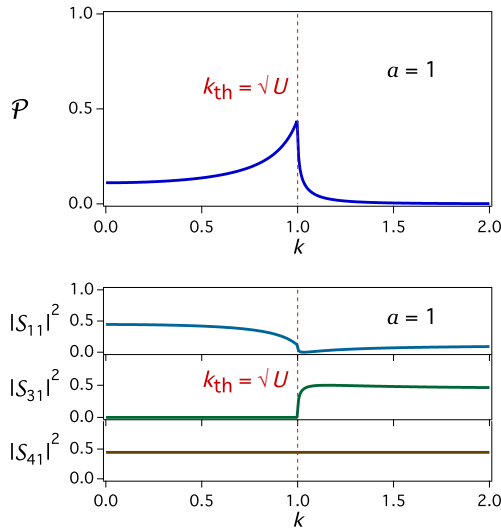


Fig. 9. Scattering characteristics of the graph from Fig. 8 with parameter $a = 1$. The transmission probability $\mathcal{P}(k; U)$ as a function of k with the value of the potential set to $U = 1$ is plotted in the top figure. The lower figure shows the reflection probability $|S_{11}(k; U)|^2$ and the probabilities of transmission to the controlling line $|S_{31}(k; U)|^2$ and to the drain line $|S_{41}(k; U)|^2$.

momentum $k_{\text{th}} = \sqrt{U}$, appearing for $a > 1/\sqrt{2}$, is again related to the pole in the unphysical Riemann plane at

$$k_{\text{pol}} = \frac{2a^2}{\sqrt{(4a^4 - 1)}} \sqrt{U}. \quad (80)$$

There is a value of the parameter a that deserves a particular attention, namely $a = 1/\sqrt{2}$. For this choice of a , the peak disappears and the function $\mathcal{P}(k; U)$ becomes constant in the whole interval $(0, \sqrt{U})$;

$$\begin{aligned} \mathcal{P}(k; U) &= \frac{1}{4} & (k \leq \sqrt{U}) \\ &= \frac{1}{4} \left(\frac{1 - \sqrt{1 - \frac{U}{k^2}}}{1 + \sqrt{1 - \frac{U}{k^2}}} \right)^2 & (k > \sqrt{U}). \end{aligned} \quad (81)$$

The situation is evident in Fig. 10. This can be also regarded as the $a = 1/\sqrt{2}$ case of (35) considered in the section IV. Our device behaves as a spectral filter with a flat passband that transmits one fourth of quantum particles with momenta $k \in [0, \sqrt{U}]$ to the output, whereas particles with higher momenta are diverted to other lines, mainly to 3 and 4. The process is directly controlled by the external potential U . Note that, at this parameter value $a = 1/\sqrt{2}$, the scattering matrix without the external potential has the form

$$S = \frac{1}{\sqrt{2}} \begin{pmatrix} 0 & 0 & 1 & 1 \\ 0 & 0 & 1 & -1 \\ 1 & 1 & 0 & 0 \\ 1 & -1 & 0 & 0 \end{pmatrix}. \quad (82)$$

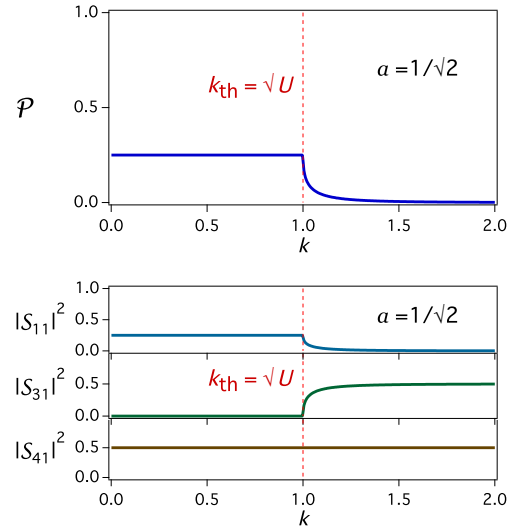


Fig. 10. Characteristics of the flat spectral filter obtained from the graph on Fig. 8 for $a = 1/\sqrt{2}$. The transmission probability $\mathcal{P}(k; U)$ as a function of k with the value of the potential set to $U = 1$ is plotted in the top figure. The lower figure shows the reflection probability $|S_{11}(k; U)|^2$ and the probabilities of transmission to the controlling line $|S_{31}(k; U)|^2$ and to the drain line $|S_{41}(k; U)|^2$.

Since increasing U opens the channel $1 \rightarrow 2$ for more particles, the device can be regarded as a *quantum sluice-gate*, applicable as a quantum flux controller (Fig. 11). When there are many particles described by the momentum distribution $\rho(k)$ on the line 1, the flux J to the line 2 is given by

$$J(U) = \int dk \rho(k) k \mathcal{P}(k; U). \quad (83)$$

Assuming the Fermi distribution with Fermi momentum k_F larger than our range of operation of \sqrt{U} , we can set $\rho(k) = \rho = \text{const}$. With the approximation $\mathcal{P}(k; U) \approx \frac{1}{4} \Theta(\sqrt{U} - k)$, we obtain

$$J(U) = \frac{1}{8} \rho U, \quad (84)$$

which indicates the linear flux control.

The sluice-gate built from an $n = 4$ star graph has another possible mode of operation. We can apply another external field V which we assume to be in the range $0 < V < U$ to the line No. 4. The local momenta on lines 1 to 4 are given by

$$k_1 = k_2 = k, \quad k_3 = \sqrt{k^2 - U}, \quad k_4 = \sqrt{k^2 - V}. \quad (85)$$

The system now has two threshold momenta given by

$$k_{\text{th1}} = \sqrt{U}, \quad k_{\text{th2}} = \sqrt{V}. \quad (86)$$

For the incoming particles from the line 1, we obtain the scattering matrix in the form

$$S_{21}(k; U) = \frac{-2a^2 \left(\sqrt{1 - \frac{U}{k^2}} - \sqrt{1 - \frac{V}{k^2}} \right)}{\left(1 + 2a^2 \sqrt{1 - \frac{U}{k^2}} \right) \left(1 + 2a^2 \sqrt{1 - \frac{V}{k^2}} \right)}, \quad (87)$$

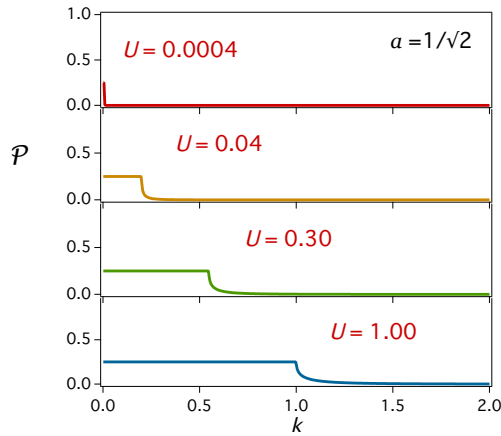


Fig. 11. The graph showing the sluice-gate operation of the quantum graph depicted in Fig. 8. The transmission spectra $\mathcal{P}(k)$ is plotted with various values of the control potential U .

$$\mathcal{S}_{11}(k; U) = \frac{1 - 4a^4 \sqrt{1 - \frac{U}{k^2}} \sqrt{1 - \frac{V}{k^2}}}{\left(1 + 2a^2 \sqrt{1 - \frac{U}{k^2}}\right) \left(1 + 2a^2 \sqrt{1 - \frac{V}{k^2}}\right)}, \quad (88)$$

$$\mathcal{S}_{31}(k; U) = \frac{2a \left(1 - \frac{U}{k^2}\right)^{\frac{1}{4}} \Theta(k - \sqrt{U})}{1 + 2a^2 \sqrt{1 - \frac{U}{k^2}}}, \quad (89)$$

$$\mathcal{S}_{41}(k; U) = \frac{2a \left(1 - \frac{V}{k^2}\right)^{\frac{1}{4}} \Theta(k - \sqrt{V})}{1 + 2a^2 \sqrt{1 - \frac{V}{k^2}}}. \quad (90)$$

The channel $1 \rightarrow 2$ opens for particles with $k \in [k_{\text{th}2}, k_{\text{th}1}]$ and mostly closes for particles with k outside this interval (Fig. 12). The gate then works as a fully tunable band spectral filter. However, in contrast to the standard $V = 0$ operation mode, the filter with $V > 0$ does not have a flat passband.

We emphasize that the controllable filter using the threshold resonance is possible only with “exotic” Fulop-Tsutsui-type couplings in the vertices. Standard vertex couplings, namely the free and the δ -coupling, fail to work in this manner. It is essential, for the proposed designs to be experimentally realizable, that the required Fulop-Tsutsui vertices can be created using standard couplings, which themselves have a simple physical interpretation [15]. This problem has been addressed in [9] and [12], where it was proved that any Fulop-Tsutsui coupling given by b. c. with real matrices A, B can be approximately constructed by assembling a few δ -couplings. The solution for our case is shown in Fig. 13: For the $n = 3$ case (top), the δ -coupling strengths are given by $v_1 = [a(a-1) + b(b-1)]/d$, $v_2 = (1-a)/d$ and $v_3 = (1-b)/d$. For the $n = 4$ case (bottom), the strengths are $v_1 = v_2 = 2a(a-1)/d$, $v_3 = v_4 = (1-2a)/d$. The double line represents a line with a “magnetic” vector potential, which can be alternatively replaced by a line carrying the δ -coupling of strength $v_5 = -8a/d$ in its center, together with changing v_2 and v_4 to $v_2 = 2a(a-2)/d$, $v_4 = (1-4a)/d$.

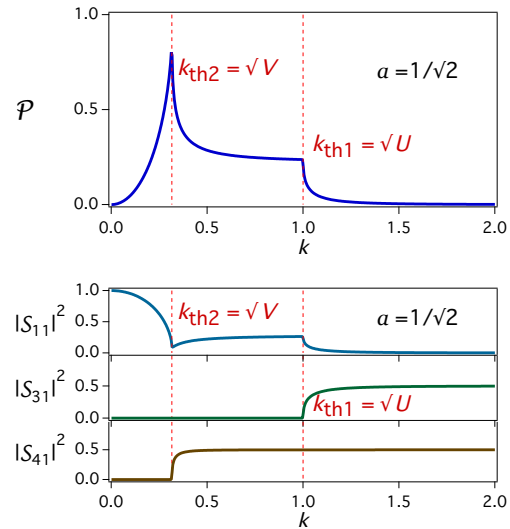


Fig. 12. Characteristics of the flat spectral filter obtained from the graph on Fig. 8 for $a = 1/\sqrt{2}$ and added second potential V on the 4th line. The transmission probability $\mathcal{P}(k; U)$ as a function of k with the value of the potentials set to $U = 1$ and $V = 0.1$ is plotted in the top figure. The lower figure shows the reflection probability $|\mathcal{S}_{11}(k; U)|^2$ and the probabilities of transmission to the two controlling lines $|\mathcal{S}_{31}(k; U)|^2$ and $|\mathcal{S}_{41}(k; U)|^2$.

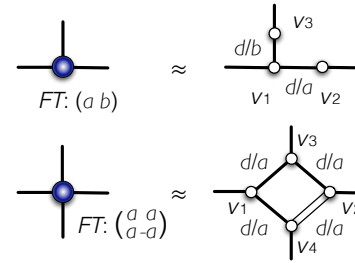


Fig. 13. Finite constructions of the Fulop-Tsutsui couplings used. The design, based on [12], utilizes the δ -couplings connected by short lines. The small size limit $d \rightarrow 0$ with the δ -coupling strengths scaled with d effectively produces the required F-T vertex coupling.

VIII. CONCLUSION AND PROSPECTS

It has been shown, in this article, that the task of finding desired property of Fulop-Tsutsui graph can be turned into mathematical problem of identifying proper Hermitian unitary matrix. Naturally, the search of system with \mathcal{S} having other interesting specifications should follow. Several questions arise along the line. One is the question whether we always have $\text{tr} \mathcal{S} = 0$ for systems with “exchange symmetric” $|\mathcal{S}_{ij}|$. The generalization to complex \mathcal{S} is also an interesting problem [16]. Other open questions include the generalization to non-Fulop-Tsutsui connection which yields general unitary \mathcal{S} not limited to Hermitian ones. The study of the bound state spectra is one thing we have completely neglected in this work. Application to non-quantum waves, including electro-magnetic wave and water wave should be another interesting subject.

Through the finite construction of star graph with no internal lines, what we have shown, in fact, amounts to the study of the low energy properties of graphs with internal lines, all of

whose edges are connected to external lines. The examination of more complicated graphs, having purely internal lines, is the natural future direction.

The full solution to the inverse scattering problem and its use as a basis for filtering device, which we have shown in this article, amount to the partial fulfillment of the hope, that quantum graph could be a solvable model and useful design tool at the same time. The application of the quantum graphs we have considered here obviously is just a starting attempt, to which many follow-ups in the future should be expected.

ACKNOWLEDGMENT

This research was supported by the MEXT, Japan under the Grant numbers 21540402 and 24540412.

REFERENCES

- [1] T. Cheon, *Reflectionless and equiscattering quantum graphs*, Proc. ICQNM 2011, Nice, France, 18–22 (2011).
- [2] M. Harmer, *Inverse scattering on metrics with boundary conditions*, J. Phys. A: Math. Theor. **38**, 4875–4885 (2005).
- [3] J. Boman and P. Kurasov, *Symmetries of quantum graphs and the inverse scattering problem*, Adv. Appl. Math. **35**, 58–70 (2005).
- [4] B. Gutkin and U. Smilansky, *Can one hear the shape of a graph?* J. Phys. A: Math. Gen. **34** 6061–6068 (2005).
- [5] P. Exner, J.P. Keating, P. Kuchment, T. Sunada, and A. Teplyaev, eds., *Analysis on Graphs and Applications*, AMS “Proceedings of Symposia in Pure Mathematics” Series, vol. 77, Providence, R.I., 2008, and references therein.
- [6] T. Fülöp and I. Tsutsui, *A free particle on a circle with point interaction*, Phys. Lett. **A264**, 366–374 (2000).
- [7] V. Kostykin and R. Schrader, *Kirchhoff’s rule for quantum wires*, J. Phys. A: Math. Gen. **32**, 595–630 (1999).
- [8] T. Cheon, P. Exner, and O. Turek, *Tripartite connection condition for quantum graph vertex*, Phys. Lett. A **375**, 113–118 (2010).
- [9] T. Cheon, P. Exner, and O. Turek, *Approximation of a general singular vertex coupling in quantum graphs*, Ann. Phys. (NY) **325**, 548–578 (2010).
- [10] T. Cheon, P. Exner, and O. Turek, *Inverse scattering problem for quantum graph vertices*, Phys. Rev. A **83**, 062715 (4pp) (2010).
- [11] P. Exner and O. Post, *Approximation of quantum graph vertex couplings by scaled Schrödinger operators on thin branched manifolds*, J. Phys. A: Math. Theor. **42**, 415305 (22pp) (2009).
- [12] T. Cheon and O. Turek, *Fulop-Tsutsui interactions on quantum graphs*, Phys. Lett. A **374**, 4212–4221 (2010).
- [13] J.M. Harrison, U. Smilansky, and B. Winn, *Quantum graphs where back-scattering is prohibited*, J. Phys. A: Math. Theor. **40**, 14181–14193 (2007).
- [14] O. Turek and T. Cheon, *Threshold resonance and controlled filtering in quantum star graphs*, arXiv.org: 1111.4775 (quant-ph) (4pp) (2011).
- [15] P. Exner, *Weakly coupled states on branching graphs*, Lett. Math. Phys. **38**, 313–320 (1996).
- [16] O. Turek and T. Cheon, *Quantum graph vertices with permutation-symmetric scattering probabilities*, Phys. Lett. A **375**, 3775–3780 (2011).